Introduction about Multislice CT and congenital heart disease

Major advances in the field of pediatric cardiology and cardiac surgery over the last several decades have led to a dramatic improvement in survival rates for most forms of congenital heart disease (CHD). For example, hypoplastic left heart syndrome, a previously lethal defect, now has early survival rates up to 90% at major centers ***(Atallah et al., 2008).***

These improved outcomes have produced a growing population of survivors with complex CHD who are now reaching adulthood . During this period, improvements in surgical and medical treatments have been accompanied by developments in diagnostic modalities ***(Gao et al., 2012).***

Since the 1980s, echocardiography has been the noninvasive imaging modality of choice for diagnosis and follow-up of children and adults with CHD and has been shown to be reliable in the diagnosis of most forms of CHD, with major diagnostic errors occurring in only 0.2% to 2% infants. New echocardiographic techniques developed in recent years, including real-time 3D echocardiography, strain/strain rate imaging, and speckle tracking, have greatly expanded the capabilities of cardiac ultrasound to evaluate anatomy and physiology of CHD ***(Dorfman et al., 2005).***

Echocardiography has replaced catheterization as the primary diagnostic modality, and it is now uncommon for newborn infants to undergo catheterization for purely diagnostic purposes. Although echocardiography remains the bedrock of noninvasive cardiac imaging, the array of diagnostic modalities and techniques available continue to grow and this has spawned the specialty of “noninvasive cardiac imaging” and the need for the “cardiac imager” to be adept in all the different modalities (***Chukwu et al., 2008).***

Currently, echocardiography is the leading diagnostic modality for the interrogation of intracardiac structures in children. However, use of this

modality is usually insufficient for the study of certain structures such as coronary arteries, extracardiac vascular anomalies, descending aorta , branches of the pulmonary artery, systemic and pulmonary venous structures ***(Wang et al., 2011).***

Diagnostic cardiac catheterization, which was associated with higher-dose radiation and longer sedation times, as well as occasional morbidity, is usually performed if echocardiography fails to provide a confident evaluation of the congenital cardiovascular lesions ***(Kaemmerer et al., 2000).***

Despite its excellent anatomic and functional assessment capabilities, magnetic resonance imaging is often limited in the evaluation of seriously-ill or uncooperative patients; its use is contraindicated for patient with pacemaker. MR imaging studies are time-consuming and may require patient sedation. So electron beam CT has been established for the evaluation of patients with congenital heart disease ***(Shen et al., 2012).***

New generation multislice CT technology has changed the approach to non-invasive assessment of congenital heart disease, in both paediatric and adult patients ***(Kroft et al., 2010).***

This is mainly because of rapid advances in spatial and temporal resolution and in post-processing capability ***(Shi et al 2013)***.

Multislice CT has seen rapid technological advances over the past 3–5 years, particularly with the recent emergence of 64-slice devices. Indeed since 2000 there has been a doubling of detector rows approximately every 2 years, with 4, 16, 32 and then 64 rows in 2004 ***(Bean et al., 2005).*** This latest technology allows much faster acquisition times, improved spatial resolution (with thinner slices) and with fewer motion artefacts, owing to improved ECG gating ***(Tuerhong and Reziwanguli, 2013)***.

CT scanning is also a valuable diagnostic tool for the diagnosis of pulmonary embolism, complex arteriovenous malformations, aneurysms, aortic dissections and even coronary arteries in certain circumstances. In such clinical

situations, CT scanning often obviates the need for conventional angiography ***(Sparrow et al., 2009).***

Three-dimensional CT imaging is particularly useful for diagnostic investigation of complex forms of congenital heart disease, preparation of complex interventional procedures involving cardiac catheterisation, and the postoperative assessment of surgical reconstructions ***(Jia et al., 2012).***

CT, including CT angiography (CTA), is important in the evaluation of congenital heart disease (CHD). It can be used for accurate depiction of complex cardiovascular anatomic features both before and after surgery and of a variety of posttreatment complications ***(Feng and Liu, 2012).***

CT facilitates the assessment of extracardiac systemic and pulmonary arterial and venous structures. It is important for cardiologists to have extensive knowledge of cardiovascular anatomy and surgical techniques ***(Gaca et al., 2008).***

Although echocardiography and catheter-directed cardiac angiography are generally accepted as the primary imaging techniques for evaluation of CHD, CT and MRI are important complementary diagnostic tools ***(Tsai et al., 2008)***.

Echocardiography may not be sufficient for evaluating extracardiac structures, such as the pulmonary arteries, pulmonary veins, the aortic arch and great vessels due to acoustic window limitations. Catheter-directed cardiac angiography is limited by its 2D nature and difficulties in simultaneous evaluation of the systemic and pulmonary vascular systems ***(Leschka et al., 2007)***.

Compared with CT, cardiac catheterization has a higher complication rate owing to its invasive nature ***(Mehta et al 2008)***, typically requires a larger volume of intravascular contrast material, more frequently requires general anesthesia ***(Hollingsworth et al., 2008)***, and often imparts greater radiation dose to the patient when appropriate pediatric CT protocols are used ***(Gaca et al., 2008).***

Advances in medicine have increased the life expectancy of patients with congenital heart disease. Thus, the population of individuals who may benefit from long-term follow-up with cross-sectional imaging is steadily increasing ***(Steiner et al., 2002).***

Cross-sectional imaging with magnetic resonance (MR) or computed tomography (CT) may help overcome the limitations of echocardiography, including a poor acoustic window and poor depiction of extracardiac vascular structures ***(Haramati et al., 2002)***, as well as limitations of conventional angiography such as overlap of adjacent cardiovascular structures, difficulties in simultaneously depicting the systemic and the pulmonary vascular systems, and catheter-related complications ***(Goo et al 2005)***.

CT has the advantages of wide spread availability and short acquisition times. The development of 64-section CT, with increased scanning speed, higher spatial resolution, and enhanced capabilities for simultaneous evaluation of cardiovascular structures and lung parenchyma, has increased the clinical application of CT for the evaluation of patients with congenital heart diseases ***(Flohr et al., 2004).***

When coupled with electrocardiographic (ECG) data, CT images accurately delineate rapidly moving cardiac and paracardiac structures and allow an assessment of coronary artery disease ***(Leschka et al., 2005)*** and associated coronary artery anomalies ***(Manghat et al., 2005)***.

In addition, 64-section CT may be used to obtain functional data about motion of the ventricular wall or cardiac valves. The modality should play a particularly substantial role in the evaluation of patients after surgical intervention for congenital heart disease ***(Peng et al., 2010)***. Its drawbacks include exposure of the patient to ionizing radiation and the risks inherent in iodinated contrast material. These disadvantages must be kept in mind when considering the use of CT, particularly in pediatric patients ***(Spevak et al 2008).***

Technical Aspects of Multislice CT in congenital heart disease

The acquisition protocols take account of the patient's age, the malformation to be studied, and the ratio of image quality to radiation dose.

Children under 5 years

This group includes neonates, infants and young children unable to achieve a 5-second breath hold and whose heart rates are high, generally above 100 beats/min. In this group of children, good image quality is difficult to obtain owing to respiratory and cardiac movement artefacts, which are all the more marked when the child is anxious or agitated ***(Goo et al., 2005)***. The rule therefore is to acquire images as quickly as possible while the child is calm or lightly sedated. This implies exploiting the speed of the CT scan along with optimal injection of contrast medium. ECG gating is avoided as it lengthens acquisition time. Contrast medium injection and image acquisition are carefully calculated to achieve optimal image quality ***(Duan et al., 2012).***

The acquisition delay is automatically determined by placing a region of interest in the aorta or pulmonary artery (depending on whether systemic or pulmonary arterial structures are to be examined), with an automatic triggering threshold at 100 HU. The contrast medium bolus is then delivered by an automatic injector to ensure that all the contrast medium passes at a sufficiently high and uniform rate during the short image acquisition period ***(Thomas and Wang, 2008).***

Injection concludes with saline rinsing of the tubes, to avoid enhancement artefacts generated by the persistence of contrast medium in the superior vena cava. Finally, radiation dose must be minimised by continuous attention to the voltage and current being applied, keeping these aspects reduced as far as possible without degrading image quality ***(Peng et al., 2010)***.

For this group of children we use the following protocol:

a- Patient preparation: sedation (oral or intrarectal pentobarbitol or chloral hydrate, or both, 30 minutes before the examination); preparation of the neonate or infant, wrapped comfortably in Velpeau strapping if necessary; insertion of a 22–24G peripheral venous line in the elbow, back of the hand or foot.

b- Scan parameters: rotation time 400 ms; high pitch 0.984, slice thickness 0.625 mm; low voltage 80 kV; current varied during acquisition and according to the weight of the child.

c- Injection parameters: volume of contrast medium (Iopamerol 300 mg/ml; Schering SA, Berlin, Germany) 1 ml/kg, followed by 5 ml saline solution; flow rate 0.5–1 ml/s for neonates; 1–2 ml/s for older children.

Children over 5 years

For this older group of children, breath holding with appropriate and sympathetic coaching is generally possible ***(Jakob et al., 2002)***. Sedation should be avoided if good cooperation from the child is required to ensure breath holding during the acquisition period. Choice of acquisition protocol depends above all on the malformation to be explored ***(Frush et al., 2005).***

Study of the great vessels (aorta, pulmonary arteries, systemic or pulmonary venous return) is relatively straightforward: it is carried out by fast acquisition times without ECG gating. Study of the coronary arteries, on the other hand, is more difficult. The best image quality is obtained with ECG-gated acquisition in a child whose heart rate is maintained stable and slow by administration of a b blocker (,70 beats/min). In all cases, the same precautions should be taken for contrast medium injection parameters and radiation dose as already described ***(Khatri et al., 2008)***.

For this group of older children we use the following protocol:

a- Patient preparation: no sedation; b blocker in the case of CT coronary angiography (propranolol, 1–2 mg/kg orally 2 hours before the examination); 20–22 G peripheral venous line in the elbow, back of the hand or foot.

b- Scan parameters:

– Examination of the great arteries: rotation time 400 ms; high pitch 0.984; slice thickness 0.625 mm; voltage 80– 100 kV depending on body weight; current varied during acquisition and adapted to the weight of the child.

– Examination of the coronary arteries: rotation time 350 ms; short pitch 0.2; slice thickness 0.625 mm; voltage 80–100 kV depending on body weight; current varied during acquisition and adapted to the weight of the child

c- Injection parameters: volume of contrast medium (Iopamerol 300 mg/ml; Schering SA, Berlin, Germany) 1.5 ml/kg maximum 70 ml, followed by 5–10 ml saline solution; high flow rate 2–3.5 ml/s.

Radiation Exposure

Particular emphasis must be placed on radiation exposure issues, because the initial CT examination in patients with congenital heart disease often takes place in childhood or in early adulthood, and repeated scanning sometimes is necessary. If ECG-gated CT is to be used, the benefits of assessing ventricular function, cardiac valves, small intracardiac abnormalities, and coronary arteries must outweigh the higher risk of radiation exposure that is inherent in the technique ***(Ben Saad et al ., 2009).***

The effective radiation dose from ECG-gated CT of the heart is estimated to be approximately 15 mSv . For comparison, the effective radiation dose from nongated CT of the chest is approximately 5 mSv. In general, three different algorithms may be used to reduce the radiation dose: First, weight-and size-based adjustments of tube current usually are performed according to the

patient's body habitus (eg, at thoracic CT, tube current is increased for the lateral projection and reduced in the anteroposterior projection) so that equal numbers of photons are received by the detector array ***(Hausleiter et al., 2006)***.

Second, an ECG-controlled tube current modulation algorithm known as ECG pulsing may be used to reduce radiation exposure by modulating the x-ray tube output according to the patient's ECG tracing ***(Gerber et al., 2005)***.

During a user-defined phase of the cardiac cycle (usually between mid- and end-diastole), the output is kept at a nominal value; in the remainder of the cardiac cycle, the tube output is reduced by 80%. The quality of low-dose images obtained during systole is sufficient for the evaluation of ventricular functional parameters or the origin and course of coronary artery anomalies; however, it is usually inadequate for the assessment of stenoses or other abnormalities in more distal parts of the coronary artery tree. Mean dose reduction rates of 29% ***(Gerber et al., 2005)*** and 37% with the use of ECG pulsing in CT coronary angiography protocols have been reported. The effective dose for ECG-gated CT scanning with ECG pulsing has been estimated as 9 mSv. Third, the radiation dose may be lowered by reducing the tube voltage. In a comparison of cardiac CT protocols in which tube voltages of 120 kV and 100 kV were used, a dose savings of 57% was found ***(Hausleiter et al., 2006)***.

Decreased tube voltage also leads to increased opacification of contrast-enhanced structures because of an increase in the photoelectric effect and decreased Compton scattering ***(Ertil-Wagner et al., 2004)***.

However, reduction of the tube voltage may result in increased image noise and decreased image quality. For noncardiac CT studies with decreased tube voltage, an increase of the tube current has been recommended to decrease image noise ***(Bean et al., 2005)***.

Although the radiation burden incurred by ECG-gated CT may be substantially reduced with dose-saving algorithms, a trade-off between a higher radiation dose and additional information provided by ECG gating must be made on a patient-by-patient basis ***(Sigal-Cinqualbre et al., 2004).***

Image processing

The acquisition volume is analysed on dedicated work stations. Routine analyses are carried out on standard slices in various planes, multiplanar and three-dimensional reconstructions. This post-processing stage is partly facilitated by vascular analysis algorithms with an interface that is interactive and simplified for the user. For CT coronary angiography, analysis is more refined and requires reconstructions at different phases of the cardiac cycle: a first set of images is obtained systematically at 75% of the R–R interval (corresponding to late diastole); further image reconstructions are performed at every 10% of the R–R interval when artefacts are present ***(Barre and paul, 2011).***

Sequential Segmental Approach

Congenital heart defects may occur in many different combinations and be very complex, and their accurate diagnosis requires profound knowledge. Several approaches to classifying congenital heart diseases have been suggested, but no consensus has been reached about nomenclature. Nomenclature systems based on embryology were common in the past; other, more physiologic classification systems rely on clinical manifestations (eg, cyanosis) and the presence of an increase or decrease in pulmonary vascularity. In the latter system, congenital heart diseases may be classified as acyanotic with increased pulmonary vascularity (with a left-to-right shunt), acyanotic with normal pulmonary vascularity (with either out-flow obstruction or valvular insufficiency), cyanotic with decreased pulmonary vascularity (with an intracardiac defect that shunts

blood away from the lung), or cyanotic with increased pulmonary vascularity (with bidirectional systemic and pulmonary venous shunts) ***(Shinebourne et al 1976).***

A simpler descriptive system derived from the sequential segmental approach was introduced in the 1980s. Based on the visualization of blood flow into, through, and out of the heart, the sequential segmental approach for interpreting anatomic images obtained in patients with congenital heart disease consists of the following steps: *(a)* determining cardiac sidedness (arrangement of atrial chambers), *(b)* locating the three segments (the atrial chambers, ventricular chambers, and the great arteries), *(c)* identifying the cardiac connections (venoatrial, atrioventricular, and ventriculoarterial), *(d)* assessing associated malformations, and *(e)* determining the cardiac position (position of the heart within the chest, orientation of the apex) ***(Anderson et al., 1984).***

The cardiac chambers are defined according to their morphologic characteristics and need not be in the expected locations. Each chamber has intrinsic morphologic features. Thus, the reader of images must be familiar with normal and abnormal morphologic features. The assessment of sidedness (situs) includes cardiac, pulmonary, and abdominal sidedness, which usually are concordant. Cardiac sidedness is determined by the position of the morphologic right atrium and is independent from cardiac position, cardiac orientation, and the positions of the ventricles or great arteries. In situs solitus (the normal configuration), the morphologic right atrium lies to the right of the morphologic left atrium. In situs in-versus, the morphologic right atrium lies to the left of the morphologic left atrium ***(Van Praagh, 1972).***

The features of congenital heart disease in adults resemble those in pediatric patients but are more likely to include complications that result from hemodynamic alterations (eg, pulmonary hypertension, ventricular hypertrophy). Therefore, changes in cardiac chamber size and morphologic

features should be thoroughly investigated with follow-up imaging studies ***(Boxt, 2004).***

Normal cardiovascular anatomy dignosed by MSCT

Knowledge of the normal cardiac morphology is a prerequisite for the evaluation of congenital heart disease ***(St. John Sutton and Rutherford, 2004).***

The heart consists of atrial, ventricular, and arterial segments. These main cardiac segments and their connections (venoatrial, atrioventricular, and ventriculoarterial) must be completely identified ***(Sigal-Cinqualbre et al., 2004).***

Atria

The appendages are landmarks for morphologic right-sidedness or left-sidedness of the atria. The right atrial appendage is characterized by a triangular shape with a broad base and a terminal crest; the left atrial appendage has a fingerlike shape with a narrow entrance (Fig 1a).

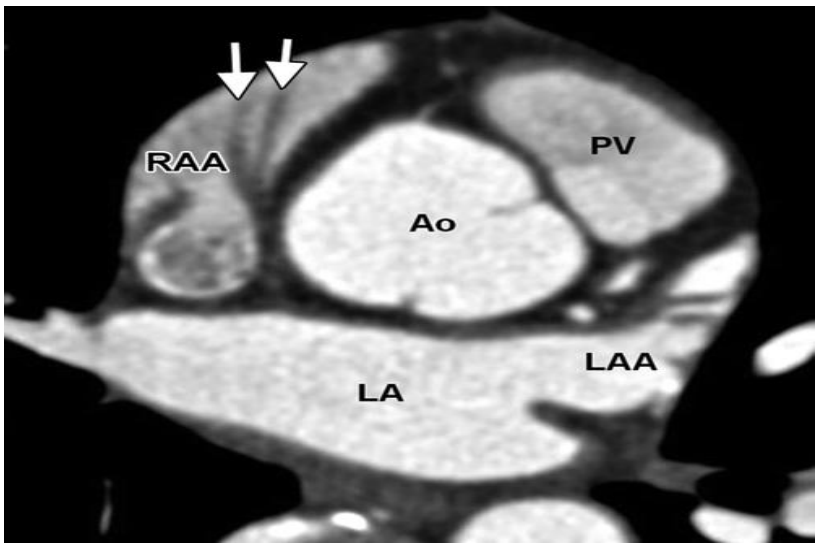

Figure 1a.Thin-section axial image at the level of the ascending aorta (Ao) and pulmonary valve (PV) demonstrates normal anatomy of the left atrium (LA) and right atrium. The right atrial appendage (RAA) typically has a triangular shape, with a wider opening and larger pectinate muscles (arrows) than those of the left atrial appendage (LAA), which has a fingerlike shape.

Ventricles

Normal ventricles consist of three components: inlet, apex, and outlet. The cornerstone for morphologic identification of the two ventricles is their inlet component, which includes the inlet (atrioventricular valve) and its tension apparatus. The latter consists of the chordae tendinae, which prevent the valve from inverting, and the papillary muscles, which are attached to the chordae tendinae and cause tension that prevents the valve from prolapsing into the atrium when the valve is closed. The inlet portion of the morphologic right ventricle is completely different from that of the morphologic left ventricle. Because the atrioventricular valve is connected to the corresponding ventricle, identification of the tricuspid and mitral valves is key for determining the ventricular structure. First, the hinge point of the tricuspid valve is more apically positioned than that of the mitral valve; second, the septal leaflet of the tricuspid valve is extensive, and its tethering to the septum is an anatomic landmark of the valve.The second landmark for determining morphologic right- or left-sidedness of ventricles is their outlet portion. The outlet of the morphologic right ventricle is a saddle-shaped supraventricular muscular crest that is located between the pulmonary valve and the tricuspid valve. There is no conical musculature between the aortic and mitral valves; instead, complete continuity of the fibrous tissue is seen (Fig 1b).

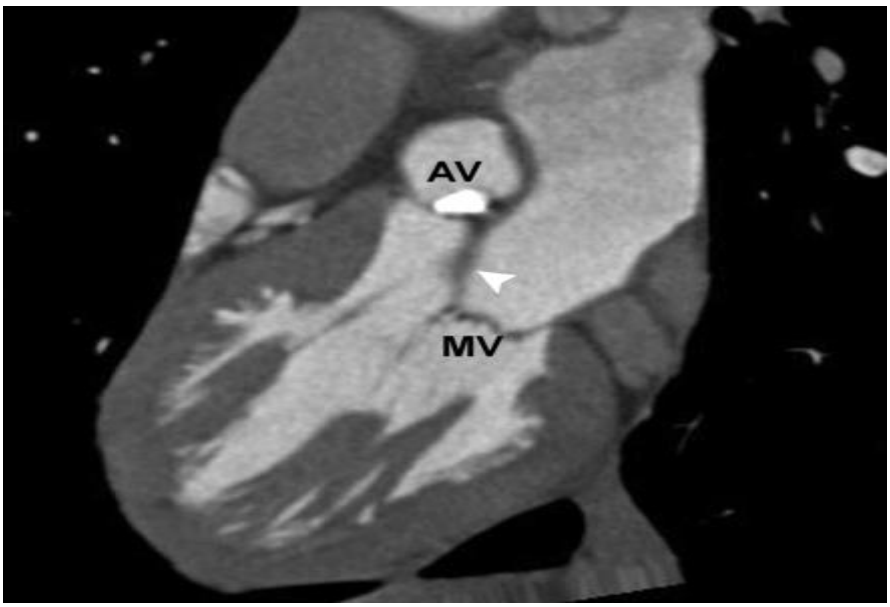

(Figure 1b) Thin-section double-oblique image through the left ventricular inflow and outflow tract shows normal anatomy of the morphologic left ventricle with fine trabeculae, the anterolateral and posteromedial papillary muscles, and fibrous continuity (arrowhead) between the aortic valve (AV) and the mitral valve (MV).

The ventricular wall thickness and the appearance of trabeculae are not useful for defining the morphologic left- versus right-sidedness of ventricles in the clinical setting. The left ventricle is demarcated by fine trabeculae and by two large papillary muscles that arise from the free wall and that are situated in the anterolateral and posteromedial positions, respectively. In the right ventricle, the muscular trabeculae are coarse and tend to parallel the right ventricular inflow and outflow tracts. The papillary muscles are relatively small and arise from both the septal and free wall surfaces. Papillary muscles that arise from the septal surface are unique to the morphologic right ventricle. Another characteristic feature of the right ventricle is the moderator band, a prominent muscle bundle that crosses from the septomarginal trabecula to the anterior papillary muscle and then to the parietal wall (Fig 1c).

(Figure 1c) Thin-section oblique sagittal image depicts the morphologic right ventricle (RV), which is characterized by coarse trabeculae and a muscular crest, the crista supraventricularis (arrowhead), between the tricuspid valve (TV) and the pulmonary valve (PV).

Great Arteries

The great arteries are distinguished by their branching pattern rather than by the arterial valve, which is indistinguishable. Connection to the morphologic right or left ventricle cannot be used to define the great arteries. In most patients, the aortic sinuses give rise to the coronary arteries. Normally, the ascending aorta arises from the left ventricle and extends to the aortic arch, which is usually on the left side and gives rise to the brachiocephalic trunk, the left common carotid artery, and the left subclavian artery. The distal part of the aortic arch, which is called the aortic isthmus and which continues as the descending aorta, gives rise to the intercostal arteries and bronchial arteries (Fig 1d).

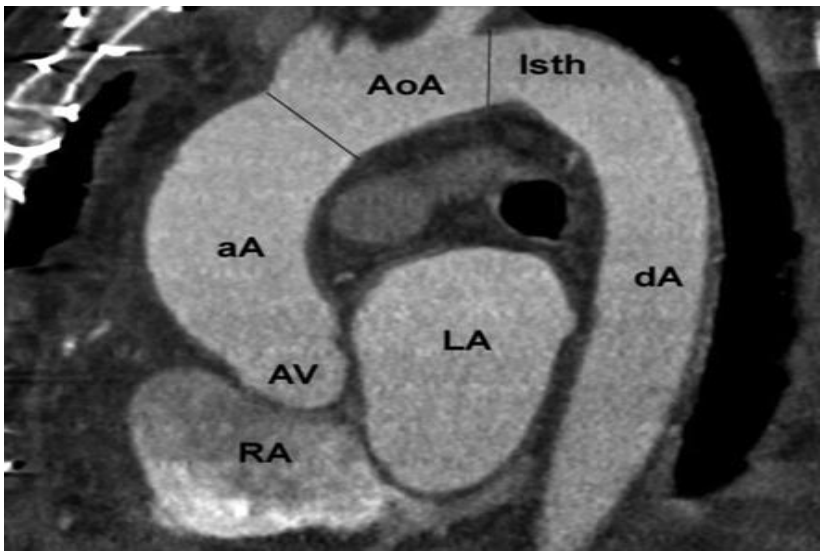

(Figure 1d) Thin-section oblique sagittal image shows the normal anatomy of the ascending aorta (aA), the aortic arch (AoA), the aortic isthmus (Isth), and the descending aorta (dA). The ascending aorta originates from the aortic valve (AV), between the left atrium (LA) and right atrium (RA).

The main pulmonary artery passes from an anterior position toward the left posterior aspect of the aorta and subdivides into the left and right pulmonary arteries. The left pulmonary artery courses in a more posterior direction, while the right pulmonary artery passes behind the ascending aorta and superior vena cava (Fig 1e).

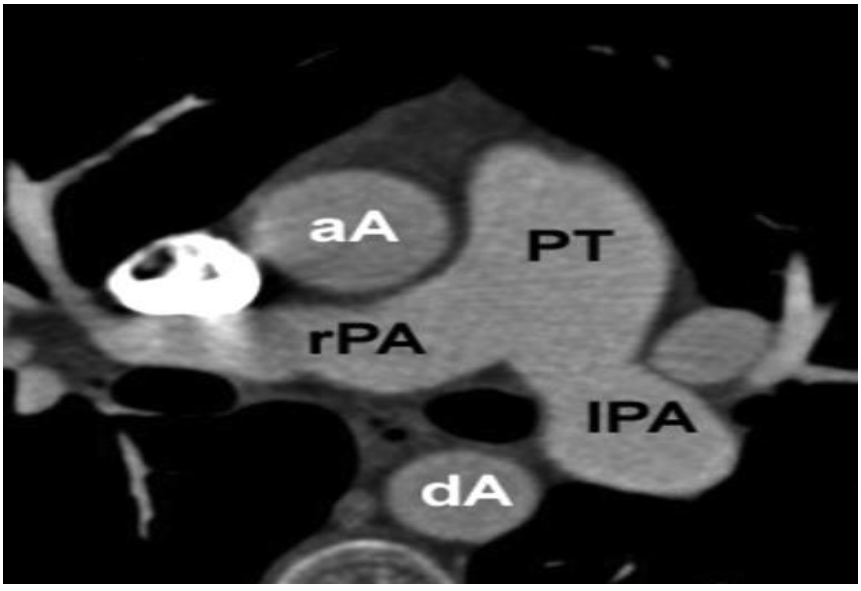

(Figure 1e) Thin-section axial image demonstrates the pulmonary trunk (PT), the left pulmonary artery (lPA), and the right pulmonary artery (rPA).

The left pulmonary artery is shorter than the right, and it courses in a more posterior direction. The right pulmonary artery passes behind the ascending aorta and the superior vena cava and in front of the descending aorta *(dA)*. The bronchial branching pattern is helpful for defining the right- or left-sidedness of pulmonary structures. However, the anatomic relationship between the upper lobe bronchus and the branch pulmonary artery is the only characteristic feature defining the morphologic left- or right-sidedness of pulmonary structures(Fig1f)

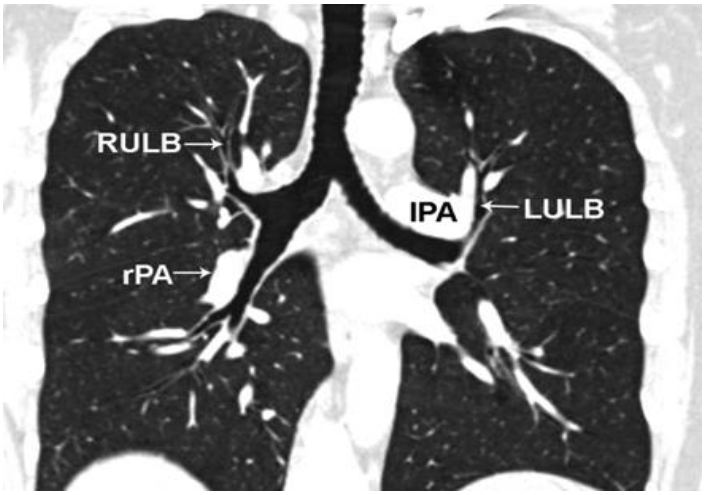

(Figure 1f) Thin-section coronal image obtained with lung window settings shows a normal bronchial branching pattern. The right upper lobe bronchus (RULB) is superior to the right pulmonary artery (rPA), whereas the left pulmonary artery (lPA) courses over the left upper lobe bronchus (LULB).

When the pulmonary structures are in the normal position (situs solitus), the right upper lobe bronchus is superior and posterior to the descending branch of the right pulmonary artery (epiarterial bronchus), while the left upper pulmonary artery courses posterior to the left upper bronchus and over the left upper lobe bronchus (hyparterial bronchus).

Great Veins

The great veins are identified by the organs that they drain. Three systemic veins are connected to the heart: the superior and inferior venae cavae and the coronary sinus (Fig 1g and Fig 1h).

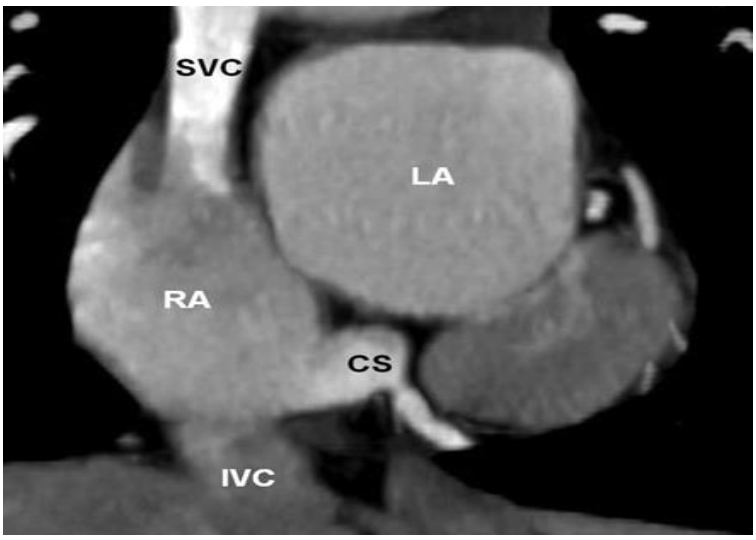

(Figure 1g) Thick-section oblique coronal image obtained with a slab thickness of 5 mm demonstrates normal connections of the three systemic veins—the superior vena cava (SVC), inferior vena cava (IVC), and coronary sinus (CS)—to the right atrium (RA). The mixture of highly contrast-enhanced venous blood from the superior vena cava with nonenhanced venous blood from the inferior vena cava is visible in the atrium. LA = left atrium.

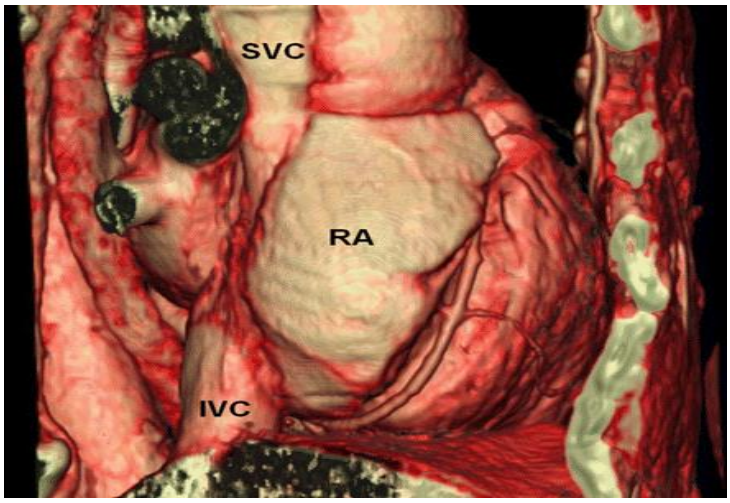

(Figure 1h) Volume-rendered image, obtained with reconstruction in an oblique right-posterior plane by using the cut-plane mode, demonstrates the relationship of the superior (SVC) and inferior (IVC) venae cavae to other anatomic structures adjacent to the site of venous connection to the right atrium (RA).

In most people, these three veins join the right atrium within the confines of the sinus venosus, which is bounded by the atrial septum and the crista terminalis.

The four pulmonary veins normally are connected to the left atrium in a different corner of the posterior atrial wall. The right upper- and middle-lobe veins join to form the right superior pulmonary vein, while the left superior pulmonary vein receives blood from the left upper lobe. The left and right inferior lobes drain blood into the left and right inferior pulmonary veins, respectively.

Examples of some complex congenital heart disease

Extracardiac Abnormalities:

Anomalous Pulmonary Venous Connection

Total anomalous pulmonary venous connection is characterized by the connection of all the pulmonary veins to the right atrium either directly or indirectly via the superior or the inferior vena cava; the pulmonary veins may form a confluence behind the left atrium ***(Ryerson and Harder, 2006)***.

Depending on the site of connection with the right atrium or systemic veins, total anomalous pulmonary venous connection is described as supracardiac, cardiac, infracardiac, or mixed ***(Goo et al., 2005)***. (Figure 2a and b)

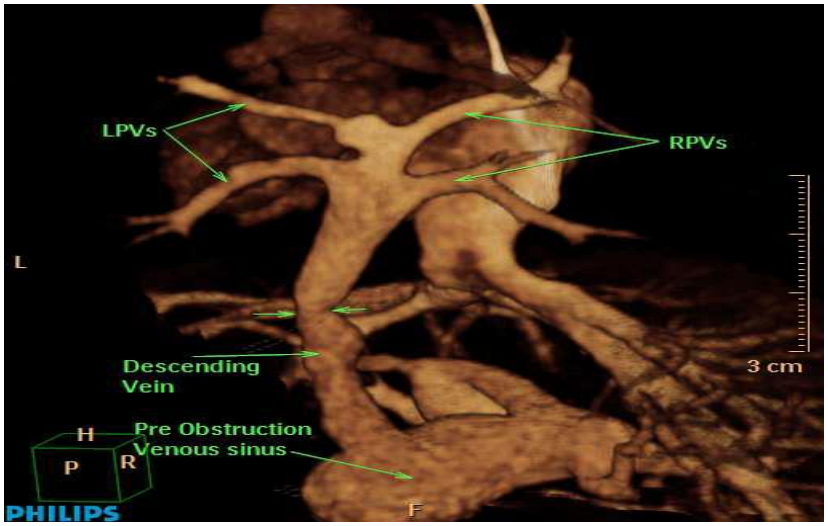

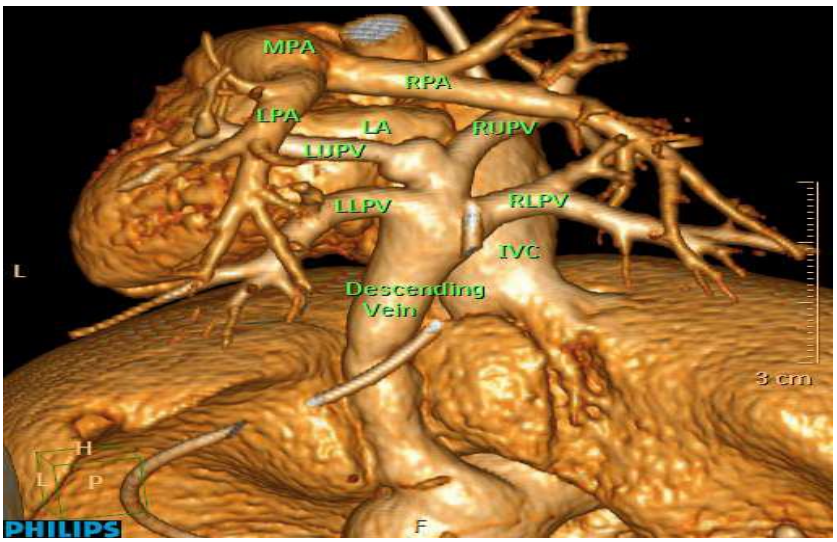

Figure 2a and b; Volume -rendered image showed infracardiac type of TAPVD

In partial anomalous pulmonary venous connection, one or more (but not all) pulmonary veins are connected to the vena cava or right atrium. The anatomic variations of partial anomalous pulmonary venous connection are manifold. Anomalous connection of the right pulmonary vein or veins to the inferior vena cava, often seen in association with hypoplasia of the right lung and anomalous systemic arterial supply through aortopulmonary collateral vessels, is called scimitar syndrome (Fig.3) ***(Kerkhoff et al., 2003).***

Abnormal connection of the right upper pulmonary vein to the superior vena cava occurs frequently in the presence of a sinus venosus defect ***(Sehgal and Loughran-Fowlds, 2005)***; in such cases, the anomalous connection occurs at a slightly higher level than it does in the absence of an interatrial communication (Fig.4). If echocardiography performed for surgical planning fails to depict the pulmonary venous connection, CT may complete the visualization of pulmonary venous connections to the atria and may provide useful information about the lung parenchyma ***(Yao et al 2011).***

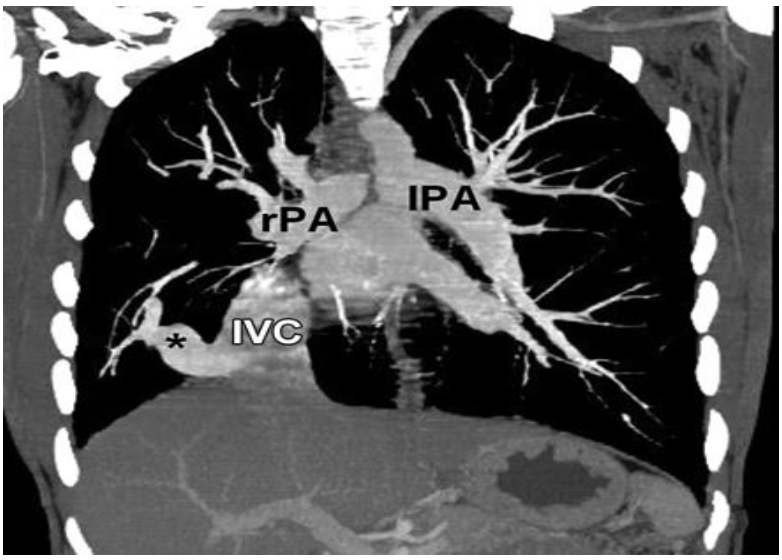

Figure 3a. Scimitar syndrome at nongated CT performed for preoperative evaluation of pulmonary structures and lung parenchyma in a 16-year-old girl. Thick-section coronal MIP image with a slab thickness of 10 mm show an anomalous connection of the right lower pulmonary vein (*) to the inferior vena cava (IVC). Hypoplasia of the right lung also is depicted. lPA = left pulmonary artery, rPA = right pulmonary artery.

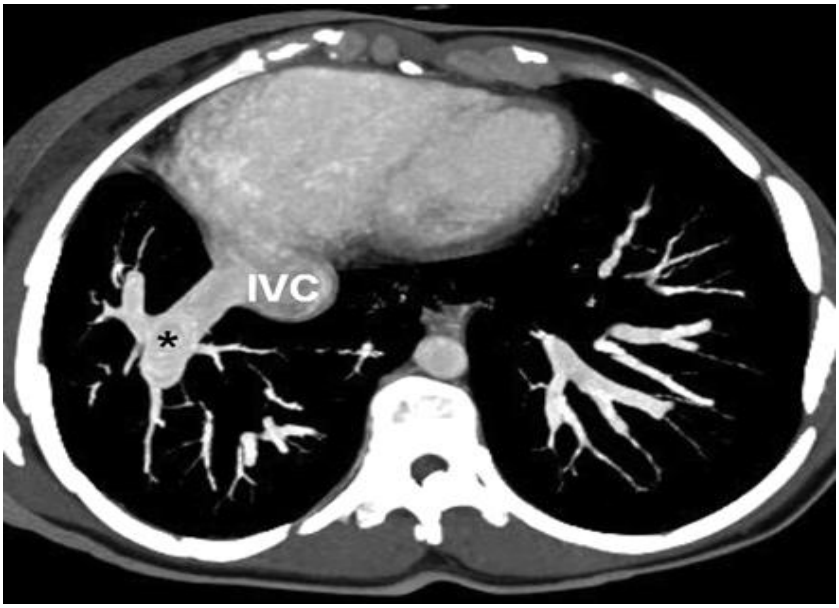

Figure 3b. Thick-section axial MIP image with a slab thickness of 10 mm show an anomalous connection of the right lower pulmonary vein (*) to the inferior vena cava (IVC). Hypoplasia of the right lung also is depicted. lPA = left pulmonary artery, rPA = right pulmonary artery.

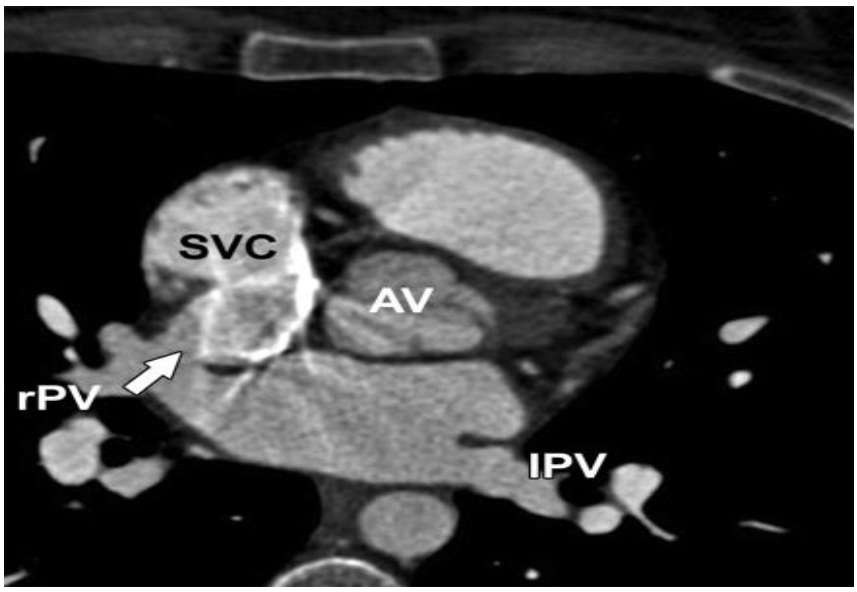

Figure 4. Partial anomalous pulmonary venous connection at ECG-gated CT performed for preoperative evaluation of coronary artery anomalies in a 37-year-old woman. Thin-section axial CT scan shows an anomalous connection of the superior right pulmonary vein (rPV) (arrow) to the right atrium via the superior vena cava (SVC). The origin and course of the coronary arteries (not shown) were normal. lPV = left pulmonary vein, AV = aortic valve.

Conotruncal Defects

Tetralogy of Fallot

This condition is characterized by a subpulmonary infundibular stenosis (which commonly coexists with an obstruction at another level), large ventricular septal defect, overriding of the aorta, and right ventricular hypertrophy (Figure 5 a,b). Several other abnormalities may occur in association with tetralogy of Fallot, including a right aortic arch in 25% of cases, an atrial septal defect in 10% of cases (so-called pentalogy of Fallot) (***(Rao et al.,1971).*** and coronary artery anomalies in another 10% of cases ***(Dabizzi et al., 1990).***

In addition, hypoplasia of the pulmonary valve and the main pulmonary artery is common. Because the surgical repair is usually performed during early childhood ***(Gaca et al., 2008),*** the role of CT in diagnosing tetralogy of Fallot is minimal. In postsurgical evaluation, the main purpose of CT is to visualize

extracardiac complications, to depict the morphologic characteristics of the main pulmonary artery and its branches (to identify any obstruction, distortion after previous palliative shunt creation, or aneurysm), and to detect any right ventricular enlargement due to chronic volume overload in the presence of severe pulmonary regurgitation ***(Taylor , 2008).***

Postsurgical evaluation is usually performed without ECG gating and with echocardiographic monitoring of ventricular function; however, ECG-gated CT should be used for the postoperative evaluation of tetralogy of Fallot if there is concern about associated coronary artery anomalies . Left and right ventricular parameters can be measured in the same study ***(Jin et al., 2011).***

Fig. 5a. Hypoplastic right ventricle in a patient with TOF. Axial CT image shows a small right ventricle in contrast with the left ventricle.

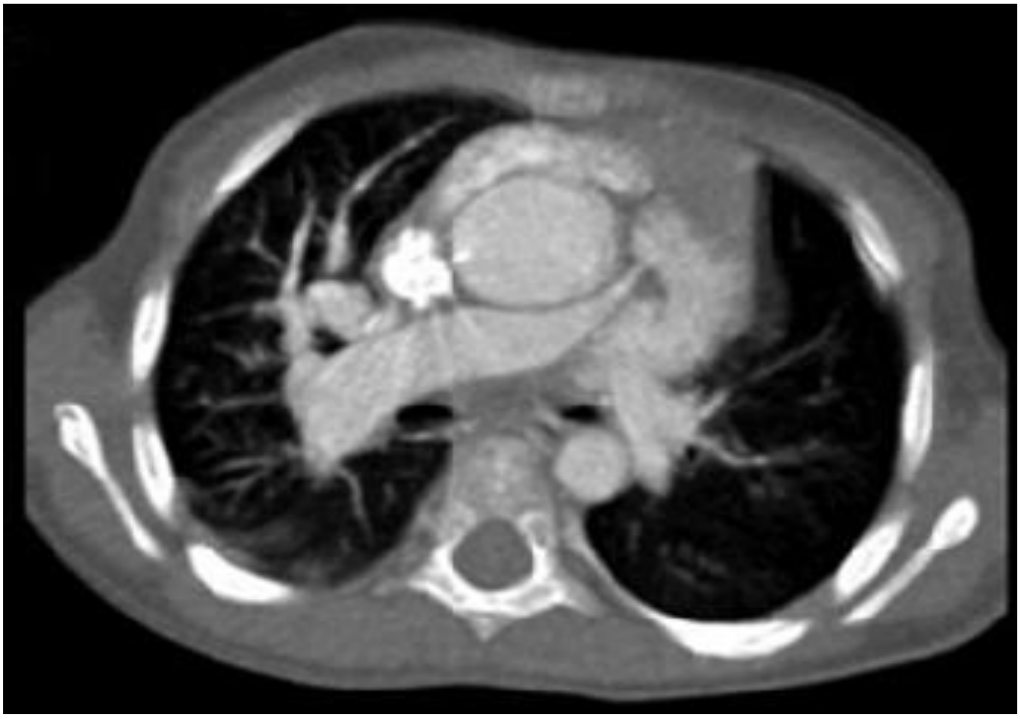

Fig. 5b. Three-year-old girl with severe pulmonary stenosis as a component of Tetralogy of Fallot (TOF).

Pulmonary Atresia

When pulmonary atresia with VSD is seen with atrioventricular and ventriculoarterial concordance, the lesion shows the morphologic characteristics of extreme form of tetralogy of Fallot . There is no pulmonary blood flow from either ventricle. Detailed morphologic evaluation of the central pulmonary artery and various pulmonary arterial feeding vessels is important for surgical planning (Figure 6 a, b and c). The central pulmonary artery may be either absent or present, and the branch pulmonary arteries may be either confluent or nonconfluent. The source of pulmonary blood flow may be multifocal, with a PDA or major aortopulmonary collateral vessels that supplement or replace primary pulmonary arterial blood flow. This source of pulmonary blood flow significantly affects the condition of the pulmonary vasculature and parenchyma ***(Geva et al ., 2002)***.

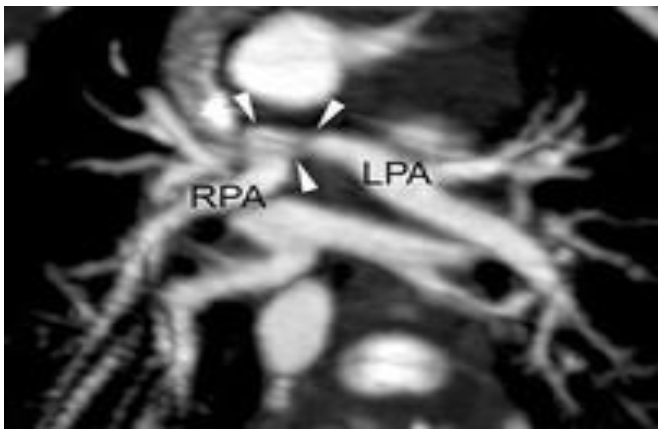

Figure 6a. Pulmonary atresia with VSD. LPA = left pulmonary artery, RPA = right pulmonary artery. CT scan shows the confluent portion of the central pulmonary artery (arrowheads).

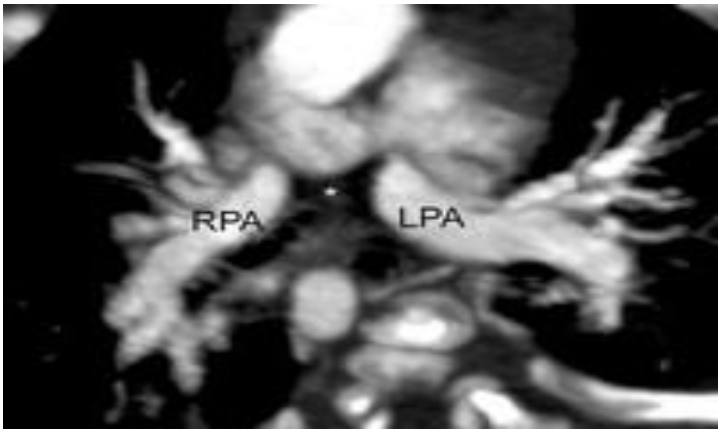

Figure 6b. CT scan shows absence of the confluent portion of the central pulmonary artery (*). Each pulmonary artery was supplied by a corresponding PDA (not shown).

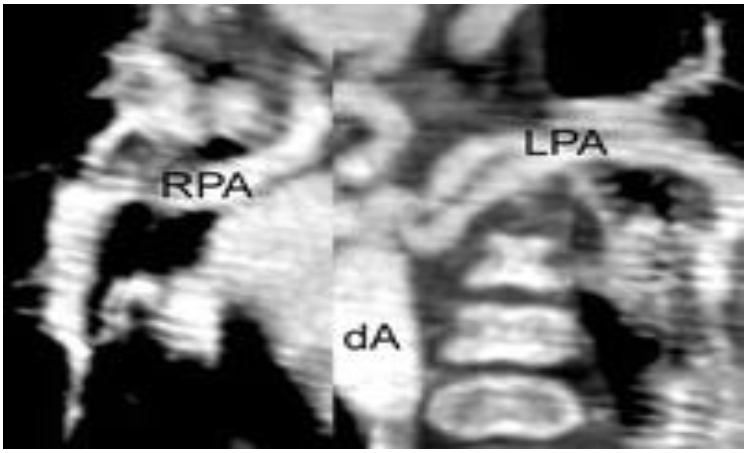

Figure 6c. CT scans depict the major aortopulmonary collateral vessels that supply the branch pulmonary arteries. These collateral vessels arise from the descending thoracic aorta (dA).

Common Arterial Trunk

Truncus Arteriosus

In this condition, a single large artery (arterial trunk) originates from the base of the heart with a single semilunar valve (truncal valve) ***(Goo et al., 2005).***

It divides into four types ***(Jacobs, 2000)***. In type 1, septum divides the origin of the aorta and pulmonary trunk. In type 2 the right and left pulmonary arteries are close to each other but arise from the trunk separately from posterior aspect of the trunk. In type 3, the right and left pulmonary arteries arise from lateral aspect of the trunk. In type 4, no pulmonary artery arises from the aorta but branches from the descending thoracic aorta supply pulmonary vasculature as multiple aortopulmonary collaterals (MAPCA) ***(Lim et al., 2002).***

All types of truncus arteriosus are always associated with VSD. About one-third of patients with a common arterial trunk also have a right-sided aortic arch. Surgical repair consists of *(a)* disconnection of the pulmonary trunk from the ascending aorta with patch closure and *(b)* restoration of continuity between the right ventricle and pulmonary vascular bed with graft implantation***(Goo et al., 2005)***.(Fig. 7, 8a and b).

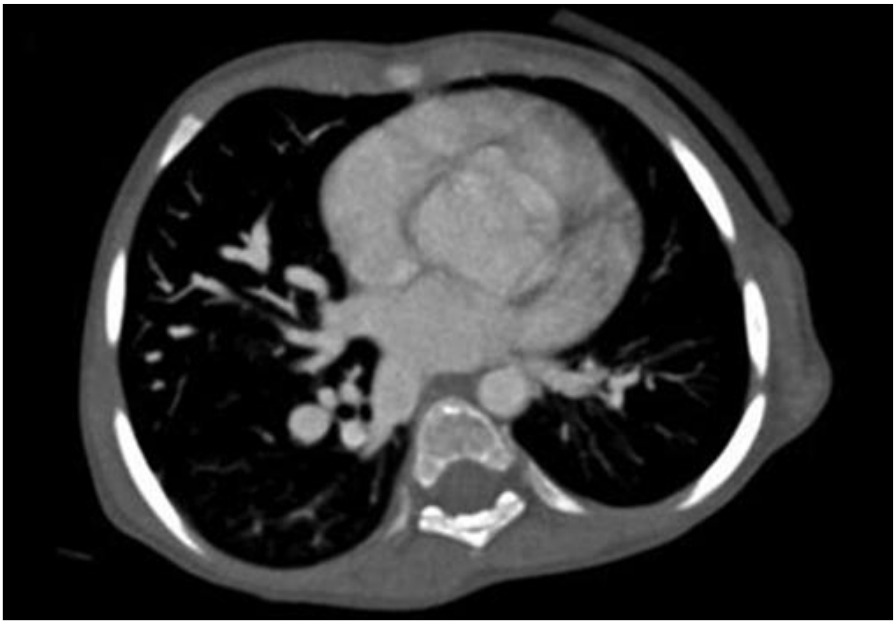

Fig. 7 . Truncus arteriosus in axial CT image reveals a single trunk above the ventricles without any pulmonary artery trunk

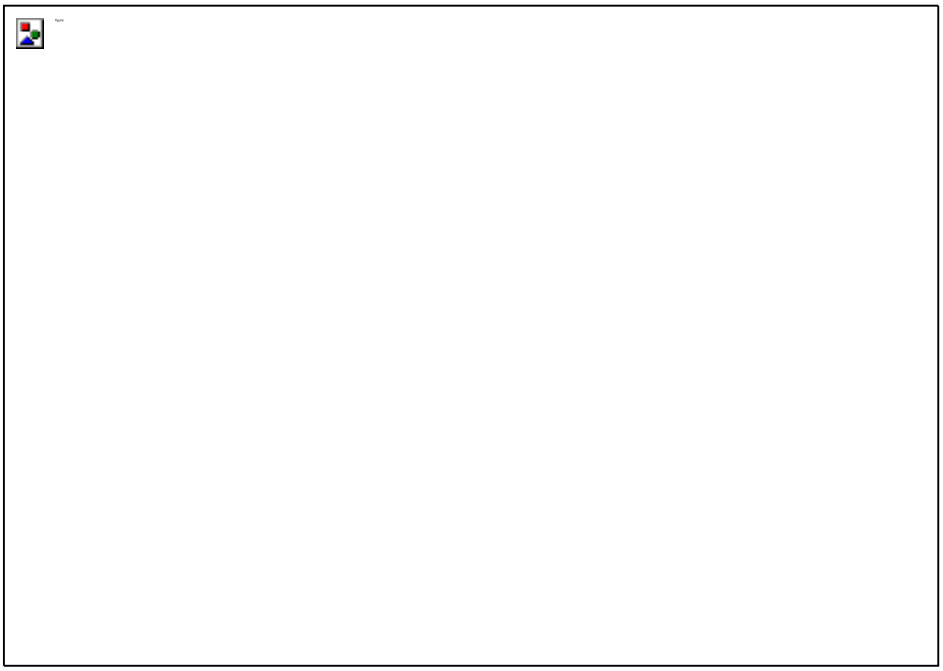

Figure 8a. Childhood surgical repair of a common arterial trunk at ECG-gated CT performed in a 32-year-old woman because of suspicion of a coronary artery anomaly. Thin-section axial CT scan shows a patch (arrow) between the common arterial trunk (CAT) and the right ventricle (RV). RA = right atrium. The connection to the ascending aorta (aA) was closed with a patch (arrow). The origin and course of the coronary arteries (not shown) were normal. dA = descending aorta, rPA = right pulmonary artery.

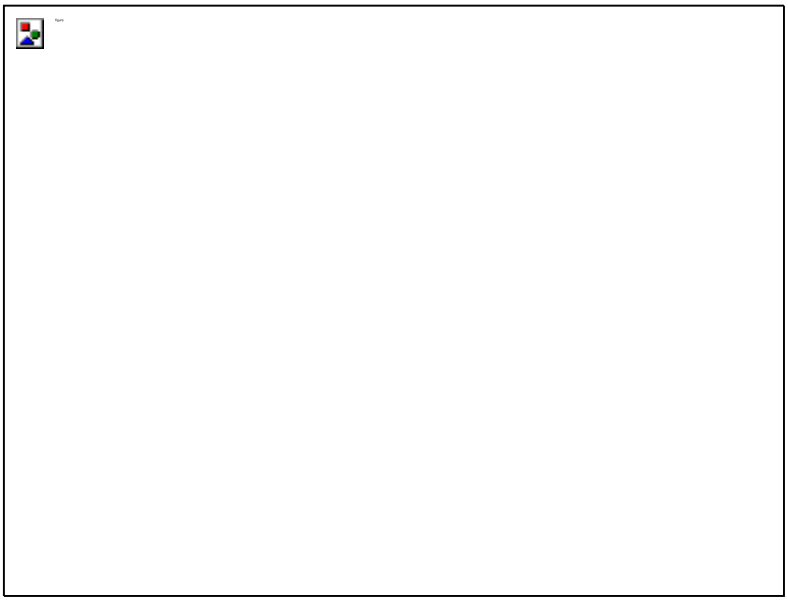

Figure 8b. Thin-section axial CT scan demonstrates a graft implanted from the right ventricle to the pulmonary trunk. The connection to the ascending aorta (aA) was closed with a patch (arrow). The origin and course of the coronary arteries (not shown) were normal. dA = descending aorta, rPA = right pulmonary artery.

Abnormal Connections: Univentricular Heart

This condition is characterized by a single atrioventricular connection, with both atria emptying into a single common ventricle (double inlet) that is morphologically predominantly left, predominantly right, or indeterminate ***(Ritter et al., 1979).***

There is a subpulmonary or subaortic outlet chamber or a rudimentary and incomplete ventricle that lacks an inlet portion. The terminology is subject to debate: A ventricular chamber that has no connection to an atrioventricular valve is usually called the outlet chamber because a ventricle is defined by an atrioventricular connection (Fig. 9a and b). A univentricular heart may be observed in association with other cardiac abnormalities and with any arrangement of the great arteries ***(Ou et al., 2007).***

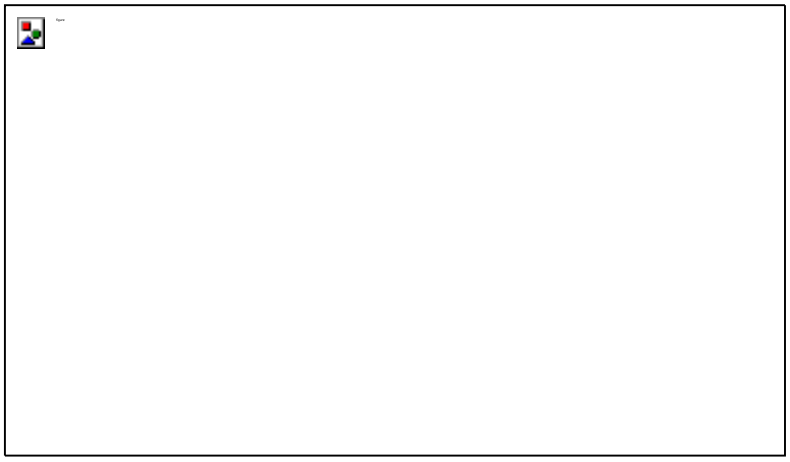

Figure 9a. Double inlet left ventricle with d-transposition of the great arteries, observed at ECG-gated CT performed to supplement postoperative echocardiography in a 30-year-old man after surgical banding of the common pulmonary artery. Thin-section reformatted image along the long axis of the heart shows connection of the left atrium (LA) and right atrium (RA) through a left-sided valve (LSV) and a right-sided valve (RSV), respectively, to a dominant ventricle (DV, morphologic left ventricle). There is no atrioventricular connection to the subaortic outlet chamber. Banding of the common pulmonary artery was performed to protect the lung from high systemic blood flow and pressure. The great arteries are in parallel position (d-transposition): The pulmonary artery arises from the morphologic left single ventricle, and the aorta arises from the subaortic outlet chamber. AV = aortic valve, PV = pulmonary valve.

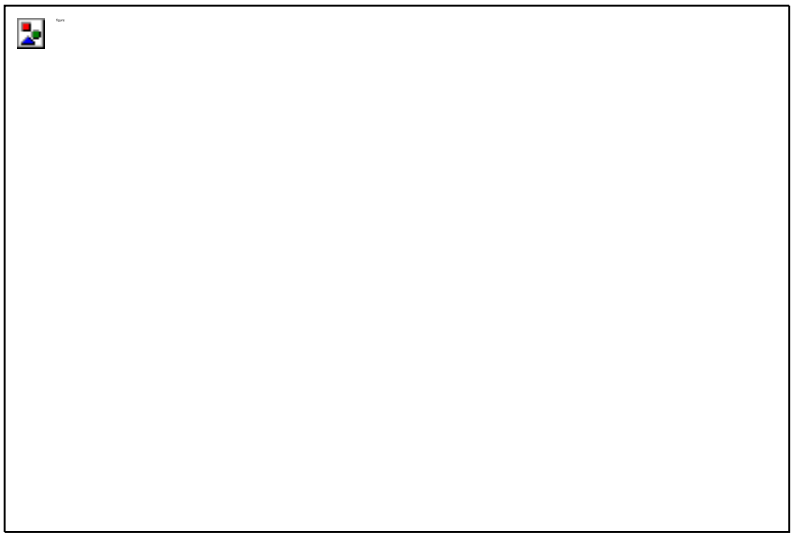

Figure 9b. Thin-section oblique sagittal image demonstrates a subaortic outlet chamber (SOC) connected via a bulboventricular foramen (*) to the subpulmonary ventricle. There is no atrioventricular connection to the subaortic outlet chamber. Banding of the common pulmonary artery was performed to protect the lung from high systemic blood flow and pressure. The great arteries are in parallel position (d-transposition): The pulmonary artery arises from the morphologic left single ventricle, and the aorta arises from the subaortic outlet chamber. AV = aortic valve, PV = pulmonary valve.

Transposition of the Great Arteries

Complete transposition of the great arteries is one of the most common types of cyanotic congenital heart disease. It is defined by concordant atrioventricular and discordant ventriculoarterial connections ***(Kawano et al., 2000).***

The aorta arises in an anterior position from the morphologic right ventricle, and the main pulmonary artery arises from the morphologic left ventricle; as a result, there is a complete separation of the pulmonary from the systemic circulation (Fig. 10a, b and c).

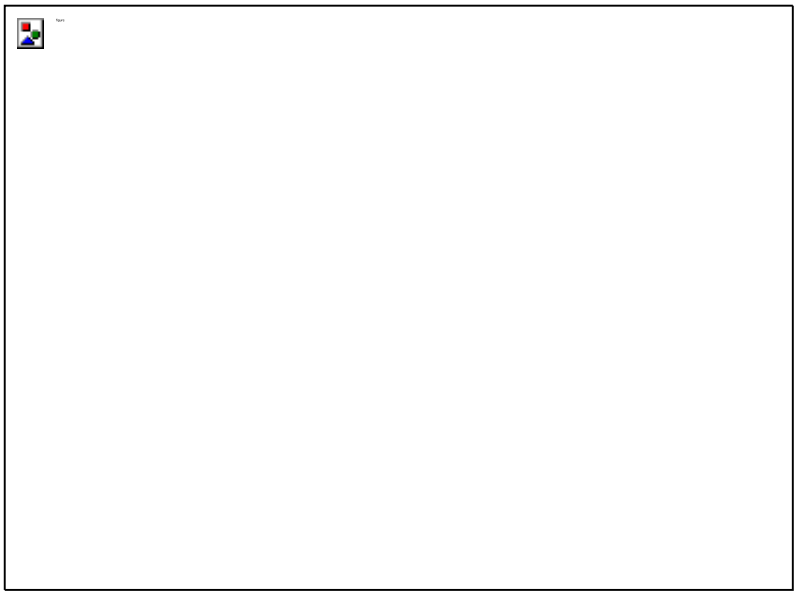

Figure 10a. Transposition of the great arteries at ECG-gated CT after an arterial switch operation and reconstruction of the atrial septum in a 17-year-old girl with a previous atrial switch procedure. CT was performed to exclude stenosis of the reimplanted coronary arteries. Thin-section axial CT scan shows the ascending aorta (aA) after its transfer by means of the LeCompte maneuver from an anterolateral position (*) to a position posterior to the pulmonary trunk (PT). As is typical after this procedure, the ascending aorta appears to be embraced by the left pulmonary artery (lPA) and right pulmonary artery (rPA). The dilated right pulmonary artery compresses the superior vena cava (SVC). A stent was implanted into the superior vena cava to relieve the obstruction of blood flow. dA = descending aorta.

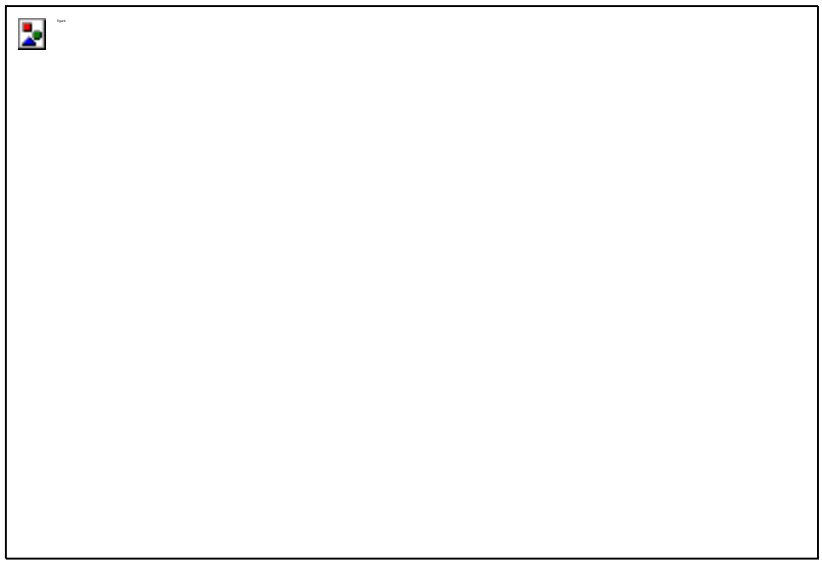

Figure 10b. Thin-section oblique coronal image shows the former aortic root in the anterior position (*) and the pulmonary trunk (PT) embracing the repositioned ascending aorta (aA). IVC = inferior vena cava, LA = left atrium, RA = right atrium.

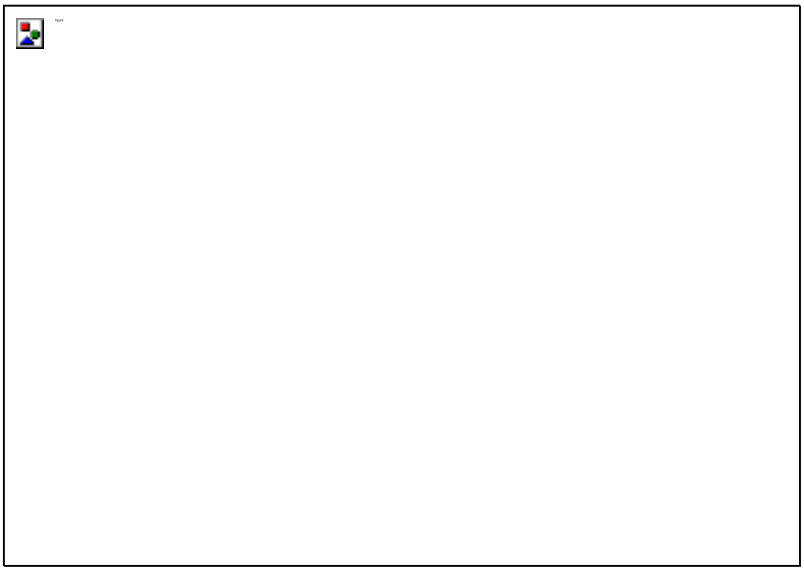

Figure 10c. Thin-section oblique sagittal image shows the postsurgical location of the ascending aorta (aA) posterior to the pulmonary trunk (PT), which is dilated and compresses the aorta. RV = right ventricle.

The pulmonary valve is in fibrous continuity with the mitral valve. In about two-thirds of patients, no other cardiac defects are present, and the patent ductus arteriosus and the patent foramen ovale ensure communication between the two circulatory pathways and survival during the first days of life. The one-third of patients with associated defects that allow intracardiac mixing (eg, atrial septal defect, ventricular septal defect) are less critically ill but are at risk for ventricular failure due to volume overload from a left-to-right shunt. Today, surgical repair is usually performed by using the arterial switch procedure, which has replaced both the Senning and the Mustad atrial switch operations ***(Siegel et al., 2005).***

However, most adults with transposition of the great arteries have undergone the atrial switch procedure, in which an atrial baffle redirects systemic venous blood to the anatomic left pulmonary ventricle and pulmonary venous blood to the anatomic right systemic ventricle, with a resultant functional atrial switch. The Mustad operation usually is performed with pericardial tissue

or a tissue graft used for the baffle, whereas in the Senning procedure the atrial septum is reconstructed to form the baffle ***(Shen et al., 2012)***.

In the arterial switch operation, the aorta and the pulmonary artery are transected above the valves and moved to the correct circulatory position. The coronary arteries are excised from the right side with a buttonlike margin of tissue around each artery and are implanted just above the valve on the left side of the heart; the areas from which the coronary arteries were excised then are patched with pericardium ***(Amat et al., 2011).***

Postoperative evaluation after an atrial switch procedure may be difficult with echocardiography because of the retrosternal position of the pulmonary trunk and pulmonary arteries. Dilatation of the great arteries and pulmonary artery stenosis are common in these patients, and nongated CT may be helpful in the evaluation of these complications ***(Lee et al 2006).***

In addition, ECG-gated CT may depict stenoses of the reattached coronary arteries after an arterial switch operation. ECG-gated CT also may be used for follow-up monitoring of ventricular function if the use of echocardiography is limited by a poor acoustic window ***(Dillman and Hernandez, 2009)***

Congenitally Corrected Transposition of the Great Arteries

In this condition, there is both an atrioventricular and a ventriculoarterial discordant connection, or double discordance . The right atrium is connected via the mitral valve to the morphologic left ventricle and then to the pulmonary artery (Fig. 11a and b). In patients with congenitally corrected transposition, the great arteries are parallel (side-by-side arrangement). In the absence of associated anomalies (eg, ventricular septal defect, pulmonary outflow tract obstruction), congenitally corrected transposition of the great arteries is often asymptomatic until adulthood. The diagnosis may be established with

echocardiography or, when echocardiographic findings are in doubt, with CT. The measurement of ventricular functional parameters at ECG-gated CT is helpful in the follow-up of these patients ***(Chen et al.,1998).***

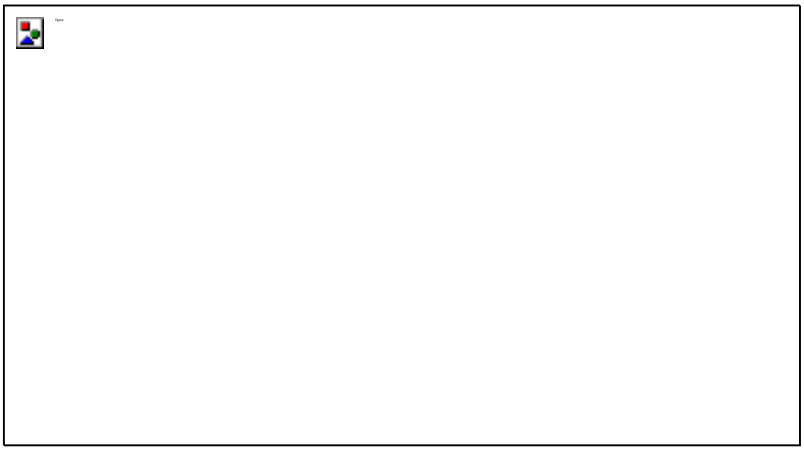

Figure 11a. Congenitally corrected transposition of the great arteries at nongated CT performed to exclude Kartagener syndrome in a 36-year-old man with known dextrocardia and chronic dyspnea. Thin-section axial CT scan shows the ascending aorta (aA) in a position anterior to and left of the pulmonary artery (PA). dA = descending aorta. The right atrium, which received flow from the systemic veins, was connected to the morphologic left ventricle (not shown). Thus, the findings included atrioventricular and ventriculoarterial discordant connections. Bronchiectasis indicative of Kartagener syndrome was not found.

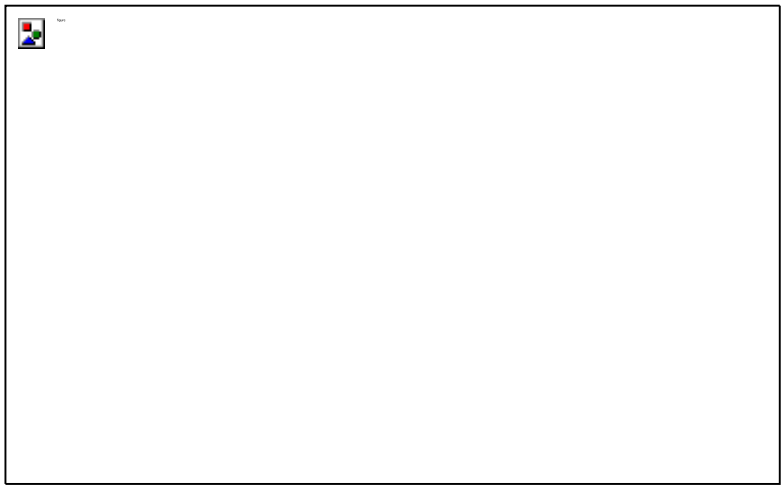

Figure 11b. Thin-section axial CT scan at the level of the ventricle shows that the pulmonary artery arises from the left ventricle (LV) and the aorta arises from the right ventricle (RV). The right atrium, which received flow from the systemic veins, was connected to the morphologic left ventricle (not shown). Thus, the findings included atrioventricular and ventriculoarterial discordant connections. Bronchiectasis indicative of Kartagener syndrome was not found.

Double Outlet Ventricle

Double outlet ventricle encompasses a wide spectrum of congenital heart abnormalities in which both great arteries arise predominantly from either the morphologic right or the morphologic left ventricle (Fig. 12a, b and c) ***(Niezen et al., 1999).***

The "50% rule" usually is applied in determining a ventriculoarterial connection, and an artery is considered to be connected to a ventricle when more than half of its semilunar valve is connected to that ventricle. In more than 50% of patients with a double outlet ventricle, both the ascending aorta and the pulmonary trunk arise from the morphologic right ventricle, a condition denoted by the term *double outlet right ventricle* ***(Ueda and Becker,1985).***

In patients with double outlet right ventricle, numerous anatomic and physiologic variations may occur with regard to the location of the ventricular septal defect (subaortic, subpulmonary) and the presence or absence of right ventricular outflow tract obstruction. The identification of anatomic and physiologic variations has an important influence on the surgical strategyECG-gated CT might be performed for the initial evaluation of these patients, to better define the position of the ventricular septal defect. However, follow-up evaluation usually is performed with nongated CT ***(De la Cruz et al., 1992).***

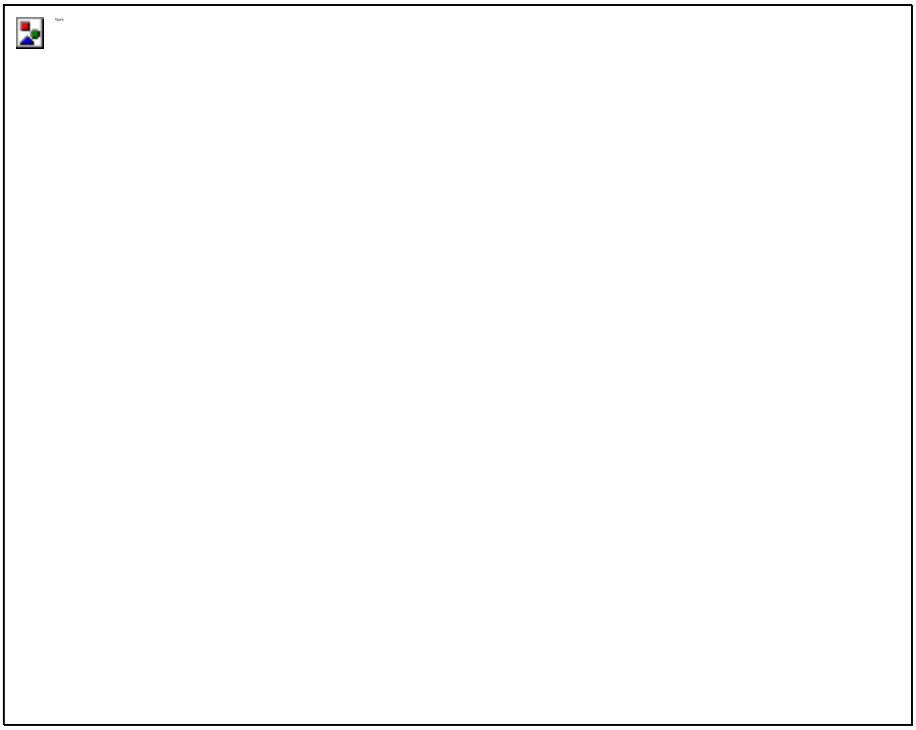

Figure 12a. Double outlet right ventricle with d-transposition of the great arteries at ECG-gated CT performed for follow-up evaluation of complex anatomy in a 17-year-old girl after a Damus-Kaye-Stansel procedure, patch closure of an atrial septal defect and tricuspid valve, and a Fontan-Kreutzer procedure. Thin-section oblique coronal image shows the connections of the systemic veins to the dilated right atrium (RA), which was surgically anastomosed to the left pulmonary artery (lPA) and right pulmonary artery (rPA). The tricuspid valve was closed with a patch. In the postsurgical circulation, blood flows directly from the systemic veins to the pulmonary arteries, without a subpulmonary ventricle (Fontan-Kreutzer procedure). The pulmonary veins are connected to the left atrium, which is connected to the hypoplastic left ventricle. The morphologic left ventricle is connected to the morphologic right ventricle (RV) via a ventricular septal defect. Both the ascending aorta (aA) and the pulmonary trunk (PT) arise from the morphologic right ventricle, with the pulmonary trunk overriding the ventricular septal defect. The pulmonary trunk was surgically connected to the ascending aorta with the Damus-Kaye-Stansel procedure. LA = left atrium.

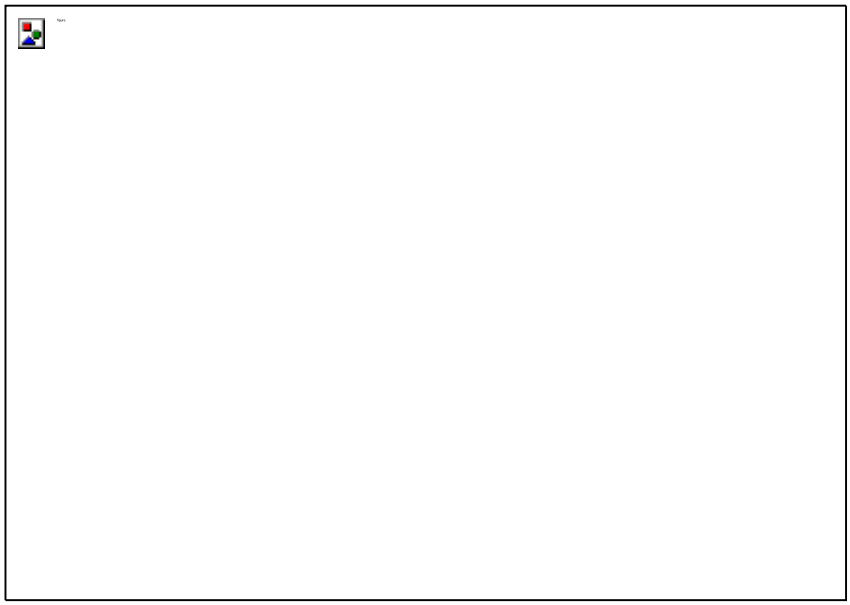

Figure 12b. Thin-section oblique sagittal image demonstrates connection of the right ventricle (RV) to the left ventricle (LV) via a ventricular septal defect (*). Both the ascending aorta (aA) and the pulmonary trunk (PT) arise from the morphologic right ventricle, with the pulmonary trunk overriding the ventricular septal defect. The pulmonary trunk was surgically connected to the ascending aorta with the Damus-Kaye-Stansel procedure. LA = left atrium.

Figure 12c. Thin-section oblique sagittal image shows a hypoplastic morphologic left ventricle (LV) and a normal-sized right ventricle (RV). Both the ascending aorta (aA) and the pulmonary trunk (PT) arise from the morphologic right ventricle, with the pulmonary trunk overriding the ventricular septal defect. The pulmonary trunk was surgically connected to the ascending aorta with the Damus-Kaye-Stansel procedure. LA = left atrium.

Isomerism

The term *isomerism* (ie, bilateral symmetry) describes paired, mirror-image sets of normally single or nonidentical organ systems. Although atrial arrangement is characterized by the left or right morphologic characteristics of the atrial appendages, accurate identification of morphologic left- or right-sidedness may be difficult ***(Chen et al., 1998).*** In patients with right isomerism, there is bilateral right-sidedness; hence, the anomalies include bilateral morphologic right atrial appendages, bilateral bronchi (trilobed right-sided lungs), asplenia syndrome, and bilateral superior venae cavae. Conversely, left atrial isomerism describes bilateral left-sidedness and includes bilateral morphologic left atrial appendages, bilateral left bronchi (bilateral bilobed lungs with hyparterial bronchus on both sides), polysplenia, and an interrupted inferior vena cava with azygos continuation (Fig. 13a, b , c and d). Although these criteria are helpful for determining sidedness, there is considerable variation within each syndrome, and features of one syndrome also may be found in another ***(Winer-Muram and Tonkin, 1989).***

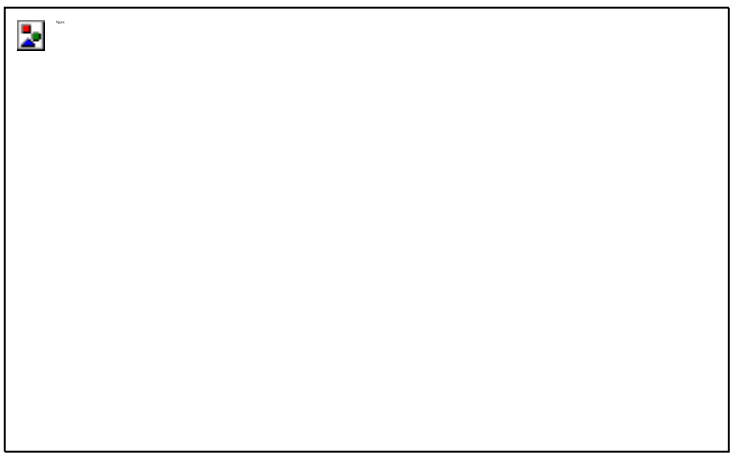

Figure 13a. Left pulmonary isomerism at ECG-gated cardiac CT and nongated chest and abdominal CT performed for suspicion of situs inversus in a 38-year-old man after unknown surgical procedures in early childhood. Thin-section reformatted image along the long axis of the heart reveals morphologic left atria on both sides, with ventricular inversion: a morphologic left atrium with right-sided pulmonary venous atrium (LA*); a morphologic left atrium with right-sided atrial appendage (LAA*); a morphologic left atrium and left-sided systemic venous atrium (LA); a morphologic left atrium and right-sided left ventricle (LV); and a morphologic right atrium and left-sided right ventricle (RV). The left-sided systemic venous atrium is connected via the tricuspid valve to the left-sided right ventricle and the pulmonary artery; the right-sided pulmonary venous atrium is connected via the mitral valve to the right-sided left ventricle and the aorta.AoA = aortic arch, AV = azygos vein, dA = descending aorta, LB = left-sided (morphologic left) bronchus, RB = right-sided (morphologic left) bronchus, SVC = left-sided superior vena cava.

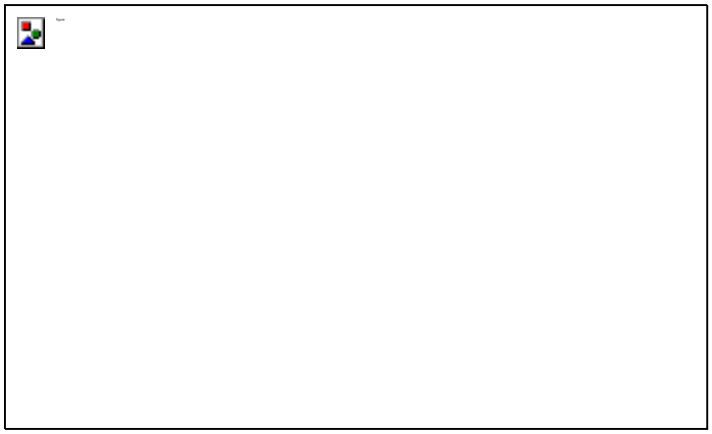

Figure 13b. Thick-section oblique coronal MIP image with a slab thickness of 10 mm shows direct connection of the hepatic veins (arrows) to the left-sided systemic venous atrium (LA). LA* = morphologic left atrium with right-sided pulmonary venous atrium, LV = left ventricle, RV = right ventricle. AoA = aortic arch, AV = azygos vein, dA = descending aorta, LB = left-sided (morphologic left) bronchus, RB = right-sided (morphologic left) bronchus, SVC = left-sided superior vena cava.

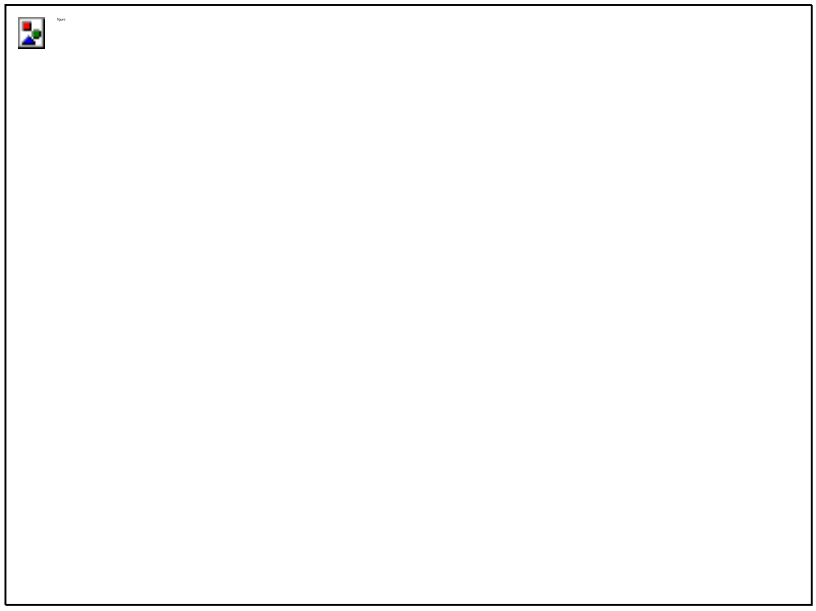

Figure 13c. Thin-section coronal reformatted image demonstrates an abnormal bronchial branching pattern, with the left pulmonary artery (lPA) and right pulmonary artery (rPA) coursing over the upper lobe bronchus on the left and right sides, respectively (hyparterial bronchus). AoA = aortic arch, AV = azygos vein, dA = descending aorta, LB = left-sided (morphologic left) bronchus, RB = right-sided (morphologic left) bronchus, SVC = left-sided superior vena cava.

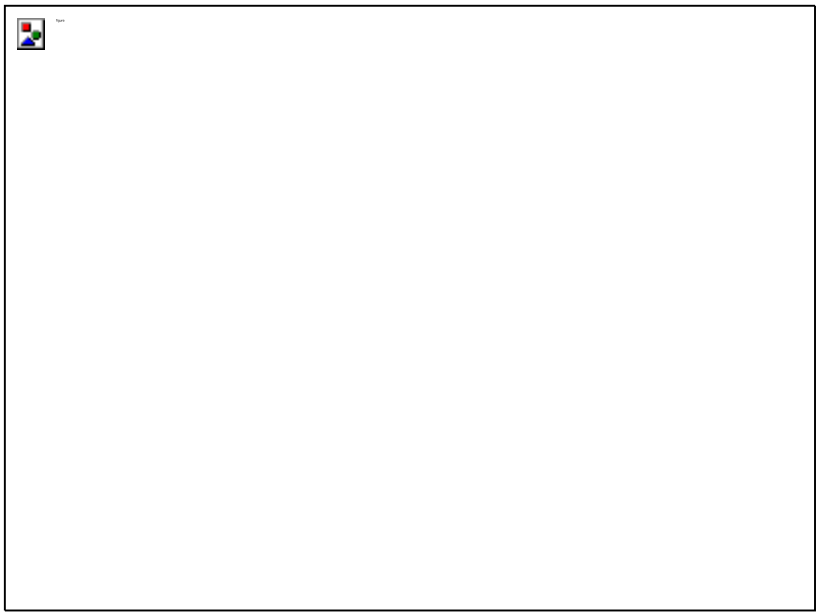

Figure 13d. Thin-section axial CT scan through the upper abdomen shows a large, predominantly midline liver and right-sided polysplenia (*). AoA = aortic arch, AV = azygos vein, dA = descending aorta, LB = left-sided (morphologic left) bronchus, RB = right-sided (morphologic left) bronchus, SVC = left-sided superior vena cava.

Conclusion

Three-dimensional imaging obtained with the latest generation of CT-scan devices represents a real advance in the morphological study of cardiovascular malformations in children and adult pre and postoperative evaluation . CT now has a vital diagnostic and decision-aiding function in the assessment of congenital heart disease, as a complement to echocardiography and more often, as a substitute for invasive angiography.

Reffrences

Anderson RH, Becker AE and Freedom RM (1984): Sequential segmental analysis of congenital heart disease. *Pediatr Cardiol*; 5: 281–287.

Amat F, Le Bret E and Sigal-Cinqualbre A (2011): Diagnostic accuracy of multidetector spiral computed tomography for preoperative assessment of sinus venosus atrial septal defects in children.Interact Cardiovasc Thorac Surg, 12(2):179-182.

Atallah J, Dinu IA, Joffe AR, Robertson CM, Sauve RS, Dyck JD, Ross DB and Rebeyka IM (2008): Two-year survival and mental and psychomotor outcomes after the Norwood procedure: an analysis of the modified Blalock-Taussig shunt and right ventricle-to-pulmonary artery shunt surgical eras. *Circulation*; *118*: *1410*–1418.

Barre E and Paul JF (2011): Segmental analysis of a complex congenital heart disease using cardiac MDCT. Analyse of congenital heart disease: use of MDCT. Arch Cardiovasc Dis, 104(1):61-63.

Bean MJ, Pannu H and Fishman EK (2005) Three-dimensional computed tomographic imaging of complex congenital cardiovascular abnormalities. *J Comput Assist Tomogr*; 29: 721–724.

Ben Saad M, Rohnean A and Sigal-Cinqualbre A (2009): Evaluation of image quality and radiation dose of thoracic and coronary dual-source CT in 110 infants with congenital heart disease. Pediatr Radiol ; 39:668–676

Boxt LM (2004): Magnetic resonance and computed tomographic evaluation of congenital heart disease. *J Magn Reson Imaging*; 19: 827–847.

Chen SJ, Li YW and Wang JK (1998): Three-dimensional reconstruction of abnormal ventriculoarterial relationship by electron beam CT. J Comput Assist Tomogr; 22: 560–568.

Chukwu EO, Barasch E, Mihalatos DG, Katz A, Lachmann J, Han J, Reichek N and Gopal AS (2008): Relative importance of errors in left ventricular quantitation by two-dimensional echocardiography: insights from three-dimensional echocardiography and cardiac magnetic resonance imaging. *J Am Soc Echocardiogr*; *21*: *990*–997.

Dabizzi RP, Teodori G, Barletta GA, Caprioli G, Baldrighi G and Baldrighi V (1990): Associated coronary and cardiac anomalies in the tetralogy of Fallot: an angiographic study. *Eur Heart J*; 11: 692–704.

De la Cruz MV, Cayre R, Arista-Salado Martinez O, Sadowinski S and Serrano A (1992): The infundibular interrelationships and the ventriculoarterial connection in double outlet right ventricle: clinical and surgical implications. Int J Cardiol; 35: 153–164.

Dillman JR and Hernandez RJ (2009): Role of CT in the evaluation of congenital cardiovascular disease in children. AJR Am J Roentgenol;192:1219 31.

Dorfman AL, Levine JC, Colan SD and Geva T (2005): Accuracy of echocardiography in low birth weight infants with congenital heart disease. *Pediatrics*; *115*: *102*–107.

Duan Yan-hua, Wang Xi-ming and Cheng Zhao-ping (2012): Application of prospective ECG-triggering dual-source CT angiography in infants and children with congenital heart disease. National Medical Journal of China, 92(3):179-183.

Ertl-Wagner BB, Hoffmann RT and Bruning R (2004): Multi-detector row CT angiography of the brain at various kilovoltage settings. *Radiology*; 231: 528–535.

Feng Chang-Zheng and Liu Lang (2012): Department of Radiology, Maternal and Child Health Hospital of Guangdong Province,Guangzhou 510010,Guangdong,China;Value of 64-detector CT with retrospective electrocardiographic gated technique for diagnosis of neonates with complexed congenital heart disease [J]; Maternal and Child Health Care of China ;19

Flohr T, Stierstorfer K, Raupach R, Ulzheimer S and Bruder H (2004): Performance evaluation of a 64-slice CT system with z-flying focal spot. *Rofo*; 176: 1803–1810.

Frush DP, Herlong JR (2005): Pediatric thoracic CT angiography. *Pediatr Radiol* ; 35:11-25.

Gaca AM, Jaggers JJ, Dudley LT and Bisset GS (2008): 3rd. Repair of congenital heart disease: a primer. Part 1. and part 2 *Radiology*; 247:617-631; 248:44-60.

Gao Y, Lu B and Hou Z (2012): Low dose dual-source CT angiography in infants with complex congenital heart disease: a randomized study. Eur J Radiol, 81(7):e789-e795.

Gerber TC, Stratmann BP, Kuzo RS, Kantor B and Morin RL (2005): Effect of acquisition technique on radiation dose and image quality in multidetector row computed tomography coronary angiography with submillimeter collimation. *Invest Radiol*; 40: 556–563.

Geva T, Greil GF, Marshall AC, Landzberg ML and Powell AJ (2002): Gadolinium enhanced 3-dimensional magnetic resonance angiography of pulmonary blood supply in patients with complex pulmonary stenosis or atresia: comparison with x-ray angiography . Circulation ; 106 : 473-478.

Goo HW, Park IS and Ko JK (2005): CT of congenital heart disease: normal anatomy and typical pathologic conditions. *RadioGraphics*; 23(Spec Issue): S147–S165.

Haramati LB, Glickstein JS, Issenberg HJ, Haramati N and Crooke GA (2002): MR imaging and CT of vascular anomalies and connections in patients with congenital heart disease: significance in surgical planning. *RadioGraphics*; 22: 337–347; discussion, 348–349.

Hausleiter J, Meyer T and Hadamitzky M (2006): Radiation dose estimates from cardiac multislice computed tomography in daily practice: impact of different scanning protocols on effective dose estimates. *Circulation*; 113: 1305–1310.

Hollingsworth CL, Yoshizumi TT and Frush DP (2008): Pediatric cardiac-gated CT angiography: assessment of radiation dose. *AJR* ; 189:12-18.

Jacobs ML (2000): Congenital Heart Surgery Nomenclature and Database Project: truncus arteriosus. Ann Thorac Surg ; 69(4 suppl): S50–S55.

Jakobs TF, Becker CR and Ohnesorge B (2002): Multi-slice helical CT of the heart with retrospective ECG gating: reduction of radiation exposure by ECG-controlled tube current modulation. *Eur Radiol*; 12: 1081–1086.

Jia Shi-jun, Jiao Jun and Wang Chun-hong (2012): Department of Radiology,the Affiliated Hospital of Guiyang Medical College,Guiyang 550004,P.R.China;Application of 320-detector row computed tomography in the diagnosis of congenital heart diseases [J] ; Radiologic Practice.

Jin Jing, Zheng Suisheng and Wang Longsheng (2011): Department of Radiology,the Second Affiliated Hospital of Anhui Medical University,Hefei 230601,China;Application value of 128-slice spiral computed tomography in preoperative assessment on tetralogy of fallot [J]; Anhui Medical Journal.

Kaemmerer H, Stern H, Fratz S, Prokop M, Schwaiger M and Hess J (2000): Imaging in adults with congenital cardiac disease (ACCD). *Thorac Cardiovasc Surg*; 48: 328–335.

Khatri S, Varma SK and Khatri P (2008): 64-slice multidetector-row computed tomographic angiography for evaluating congenital heart disease. Pediatr Cardiol ; 29:755–762

Kawano T, Ishii M and Takagi J (2000): Three-dimensional helical computed tomographic angiography in neonates and infants with complex congenital heart disease. Am Heart J; 139: 654–660.

Kerkhoff G, Albes G, Montag M, Kamler M, Jakob H and Budde T (2003): A "late" scimitar syndrome: diagnostic contribution of cardiac computed tomography [in German]. *Z Kardiol* ; 92: 595–600.

Kroft LJ, Roelofs JJ and Geleijns J (2010): Scan time and patient dose for thoracic imaging in neonates and small children using axial volumetric 320-detector row CT compared to helical; 64-, 32-, and 16- detector row CT acquisitions. Pediatr Radiol 40:294–300

Lee T, Tsai IC and Fu YC (2006): Using multidetector-row CT in neonates with complex congenital heart disease to replace diagnostic cardiac catheterization for anatomical investigation: initial experiences in technical and clinical feasibility. *Pediatr Radiol* ; 36:1273-1282.

Leschka S, Alkadhi H and Plass A (2005): Accuracy of MSCT coronary angiography with 64-slice technology: first experience. *Eur Heart J* ; 26: 1482–1487.

Leschka S, Oechslin E and Husmann L (2007): Pre- and postoperative evaluation of congenital heart disease in children and adults with 64-section CT. *RadioGraphics* ; 27:829-846.

Lim C, Kim WH, Kim SC, Lee JY, Kim SJ and Kim YM (2002): Truncus arteriosus with coarctation of persistent fifth aortic arch. Ann Thorac Surg; 74:1702-1704.

Manghat NE, Morgan-Hughes GJ, Marshall AJ and Roobottom CA (2005): Multidetector row computed tomography: imaging congenital coronary artery anomalies in adults. *Heart*; 91: 1515–1522.

Mehta R, Lee KJ, Chaturvedi R and Benson L (2008): Complications of pediatric cardiac catheterization: a review in the current era. *Catheter Cardiovasc Interv* ; 72:278-285.

Niezen RA, Beekman RP, Helbing WA, van der Wall EE and de Roos A (1999): Double outlet right ventricle assessed with magnetic resonance imaging. Int J Card Imaging ; 15: 323–329.

Ou P, Celermajer DS, Calcagni G, Brunelle F, Bonnet D and Sidi D (2007): Three dimensional CT scanning: a new diagnostic modality in congenital heart disease. Heart; 93:908—913.

Peng Keyu Liang, Hanhuan Lin Qiaochang, Zhang Hong and Zhu Peigui (2010): Deparment of Radiology,the People's Hospital of Gaozhou City,Guangdong,525200,China;Application of Multi-slice Spiral CT in Diagnosis of Children Congenital Heart Disease[J];China Modern Doctor.

Rao BN, Anderson RC and Edwards JE (1971): Anatomic variations in the tetralogy of Fallot. *Am Heart J* ; 81: 361–371.

Ritter DG, Seward JB, Moodie D and Danielson GK (1979): Univentricular heart (common ventricle): preoperative diagnosis—hemodynamic, angiocardiographic and echocardiographic features. Herz ; 4: 198–205.

Ryerson L and Harder J (2005): Totally anomalous pulmonary venous return. *Cardiol Young*; 15: 304–305.

Sehgal A and Loughran-Fowlds A (2005): Scimitar syndrome. *Indian J Pediatr*; 72: 249–251.

Shen Yan-guang1, Su Lan-fang1, Wang Yun-hua2, Huang Ting2 and Nie Zhong-shi 31 (2013): Department of Radiology, Affiliated Hospital of Hainan Medical College, Haikou 570102, Hainan Province, China; 2 Department of Radiology, the Second Xiangya Hospital of Central South University, Changsha 410011, Hunan Province, China; 3Department of Radiology, Hainan Provincial Nongken General Hospital, Haikou 570311, Hainan Province, China;Application of 64-slice spiral CT three-dimensional post-processing image for the diagnosis of the extracardiac structural anomalies [J] ;Chinese Journal of Tissue Engineering Research; 26.

Shinebourne EA, Macartney FJ and Anderson RH (1976): Sequential chamber localization—logical approach to diagnosis in congenital heart disease. *Br Heart J* ; 38: 327–340.

Shi Sheng-li, Chen Zhi-ping and Feng Dong-meng (2013): Department of Radiology,Zhengzhou Children's Hospital,Zhengzhou 450053,He'nan,China;64-Slice CT Angiography in Diagnosis of Congenital Heart Disease in Children[J] ;Chinese Journal of General Practice; 08

Siegel MJ, Bhalla S, Gutierrez FR and Billadello JB (2005): MDCT of postoperative anatomy and complications in adults with cyanotic heart disease. AJR Am J Roentgenol ; 184: 241–247.

Sigal-Cinqualbre AB, Hennequin R, Abada HT, Chen X and Paul JF (2004): Low-kilovoltage multi-detector row chest CT in adults: feasibility and effect on image quality and iodine dose. *Radiology* ; 231: 169–174.

Sparrow P, Merchant N, Provost Y, Doyle D, Nguyen E, Paul N (2009): Cardiac MRI and CT features of inheritable and congenital conditions associated with sudden cardiac death. *Eur Radiol* ; 19:259-270.

Spevak PJ, Johnson PT and Fishman EK (2008): Surgically corrected congenital heart disease: utility of 64-MDCT. *AJR*; 191:854-861.

Steiner RM, Reddy GP and Flicker S (2002): Congenital cardiovascular disease in the adult patient: imaging update. *J Thorac Imaging*2002; 17: 1–17.

St. John Sutton MG and Rutherford JD (2004): Clinical cardiovascular imaging: a comparison to Braunwald's heart disease. Philadelphia, Pa: Elsevier Saunders.

Taylor AM (2008): Cardiac imaging: MR or CT? Which to use when. *Pediatr Radiol* ; 38[suppl 3]:S433-S438.

Thomas KE and Wang B (2008): Age-specific effective doses for pediatric MSCT examinations at a large children's hospital using DLP conversion coefficients: a simple estimation method. Pediatr Radiol; 38:645–656.

Tsai IC, Chen MC and Jan SL (2008): Neonatal cardiac multidetector row CT: why and how we do it. *Pediatr Radiol* ; 38:438-451.

Tuerhong A and Reziwanguli A (2013): Department of Radiology,the Xinjiang Uygur Autonomous Region Uygur Medical Hospital;Urumqi Children's Hospital Room CT;;Use value of the 16-slice spiral CT in the diagnosis of children with congenital heart disease[J];China Medicine and Pharmacy;15.

Ueda M and Becker AE (1985): Classification of hearts with overriding aortic and pulmonary valves. Int J Cardiol ; 9: 357–369.

Van Praagh R (1972): The segmental approach to diagnosis in congenital heart disease. In: Bergsama D, ed. Birth defects. National Foundation–March of Dimes Original Articles series, vol VIII, no. 5. Baltimore, Md: Williams & Wilkins; 4–23.

Wang Hao-lu, Ye Qing, Xu Gen-xing and Xue Song (2011): Department of Thoracic and Cardiovascular Surgery, Shanghai Jiaotong University School of Medicine Renji Hospital, Shanghai 200127, China);Multislice Computed Tomography and Echocardiography in the Diagnosis of Congenital Heart Disease in Chinese Population: A Meta-Analysis[J];The Journal of Evidence-Based Medicine.

Winer-Muram HT and Tonkin IL (1989): The spectrum of heterotaxic syndromes. Radiol Clin North Am ; 27: 1147–1170.

Yao Qiong, Huxi-Hong and Pami-Er (2011) : Department of Radiology,Children′s Hospital of Fudan University, Shanghai 201102,P.R.China;64-slice CT angiography in the diagnosis of anomalous pulmonary venous drainage in children [J]; Radiologic Practice.